Preparation and characterization of mononuclear Co, Ni, and Zn complexes of dinucleating macrocyclic hexaaza-dithiophenolate ligands and their open-chain derivatives

Thorsten Fritz,[b] Gunther Steinfeld,[b] Steffen Käss[a] and Berthold Kersting*[a]

Received 13th March 2006, Accepted 9th May 2006
First published as an Advance Article on the web 19th May 2006
DOI: 10.1039/b603740b

The preparation and characterization of mononuclear complexes of the dinucleating 24-membered hexazadithiophenolate macrocycles H_2L^2 and H_2L^3 and their open-chain N_3S_2 analogues H_2L^4 and H_2L^5 are reported. The highly crystalline compounds $[Ni(L^4)]$ (**4**), $[Ni(L^5)]$ (**5**), $[Co(L^5)]$ (**6**), $[NiH_2(L^2)]^{2+}$ (**7**), $[ZnH_2(L^2)]^{2+}$ (**8**), and $[NiH_2(L^3)]^{2+}$ (**9**) could be readily prepared by stoichiometric complexation reactions of the hydrochlorides of the free ligands with the corresponding metal(II) dichlorides and NEt_3 in methanolic solution. All complexes were characterized by X-ray crystallography. Monometallic complexes **4–6** of the pentadentate ligands H_2L^4 and H_2L^5 feature distorted square pyramidal MN_3S_2 structures ($\tau = 0.01$ to 0.44). Similar coordination geometries are observed for the macrocyclic complexes **7–9** of the octadentate ligands H_2L^2 and H_2L^3. The two hydrogen atoms in **7–9** are attached to the noncoordinating benzylic amine functions and are hydrogen bonded to the metal-bound thiophenolate functions. A comparison of the structures of **4–9** reveals that the macrocycles L^2 and L^3 have a rather flexible ligand backbone that do not confer unusual coordination geometries on the metal ions. We also report on the ability of the monometallic complexes **7** and **8** to serve as starting materials for the preparation of dinuclear complexes.

Introduction

Mononuclear complexes of dinucleating macrocyclic ligands represent versatile starting materials for the preparation of heterodinuclear complexes.[1–5] The vast majority of such complexes are derived from the tetraaza-diphenolate system H_2L^1 (Scheme 1), first described by Robson *et al.*,[6] and their countless derivatives.[7–12] Far less is known about the ability of the related polyaza-dithiophenolate macrocycles to stabilize mononuclear complexes,[13–15] which can be traced to the difficulties encountered during their synthesis.[16]

Recently, we have reported the first example for a mononuclear complex of the permethylated hexaza-dithiophenolate ligand H_2L^2 (Scheme 1).[17] In this paper, we describe the synthesis and characterization of several other mononuclear complexes of this macrocycle and its per-N-propylated derivative H_2L^3. The preparations of the corresponding complexes of the open-chain chelate ligands H_2L^4 and H_2L^5 are also described and their structures are compared with those of the mononuclear macrocyclic complexes. The ability of the mononuclear complexes to serve as starting materials for homo- and heterodinuclear complexes is described briefly.

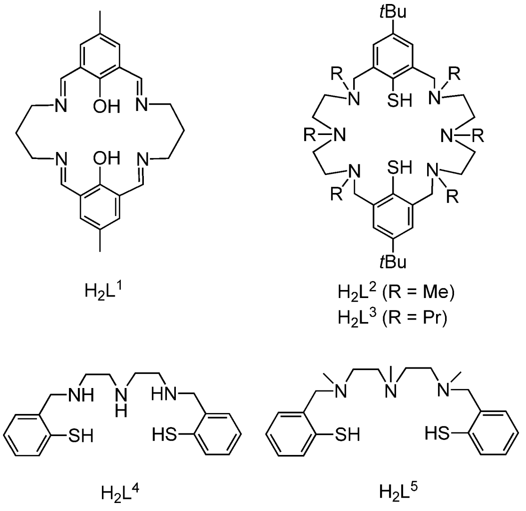

Scheme 1 Structure of the ligands H_2L^1–H_2L^5.

Results and discussion

Synthesis of ligands and complexes

The macrocycles H_2L^2,[18] and H_2L^3,[19] have been reported earlier. Scheme 2 illustrates the synthetic route to the new acyclic ligands H_2L^4 and H_2L^5.

The thioether **2** was obtained as a pale-yellow oil by a Schiff-base condensation of 2-(*tert*-butylthio)benzaldehyde **1** and bis(2-aminoethyl)amine in an ethanol/dichloromethane mixed solvent

---

[a] *Institut für Anorganische Chemie, Universität Leipzig, Johannisallee 29, D-04103 Leipzig, Germany. E-mail: b.kersting@uni-leipzig.de; Fax: +49/(0)341-97-36199*
[b] *Institut für Anorganische und Analytische Chemie, Universität Freiburg, Albertstr. 21, 79104 Freiburg, Germany*

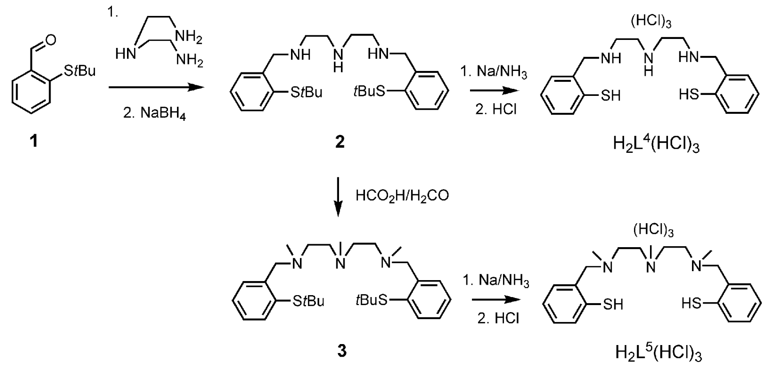

Scheme 2 Synthesis of H_2L^4 and H_2L^5.

system followed by reduction with $NaBH_4$. Reductive methylation of **2** with formaldehyde and formic acid under Eschweiler–Clarke conditions gave the permethylated derivative **3** in nearly quantitative yield. Both the unmethylated and the permethylated thioether could be converted to the corresponding thiophenols using sodium in liquid ammonia as reducing agent. Both compounds were isolated as their trihydrochloride salts and stored under an atmosphere of dry nitrogen. These acyclic ligands could not be obtained in analytically pure form. Nevertheless, they were of sufficient purity for metal complex syntheses.

The synthesis of the mononuclear complexes **4–6** is outlined in Scheme 3. Treatment of $H_2L^4{\cdot}3HCl$ with $NiCl_2{\cdot}6H_2O$ and triethylamine in a 1 : 1 : 5 ratio in methanol solution gave paramagnetic [Ni(L⁴)] (**4**) (μ_{eff} = 2.85 μ_B) as a green, air-stable, microcrystalline solid in 77% yield. The permethylated derivative $H_2L^5{\cdot}3HCl$ reacted in a similar manner to afford air-stable [Ni(L⁵)] (**5**) (μ_{eff} = 2.91 μ_B) as a red, microcrystalline solid. The dark-green, air-stable cobalt(II) complex [Co(L⁵)] (**6**) (μ_{eff} = 4.20 μ_B) was obtained in the same manner. Complexes **5** and **6** are only slightly soluble in polar protic solvents, but can be readily dissolved in polar aprotic solvents (*e.g.* MeCN, DMSO, DMF). Complex **4** is insoluble in all common organic solvents.

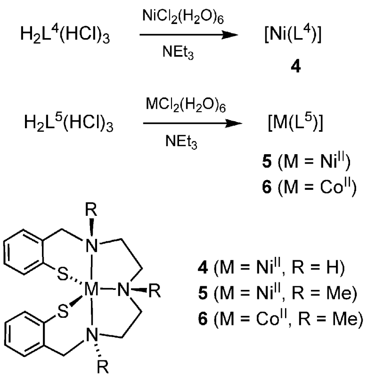

Scheme 3 Synthesis of complexes **4–6**.

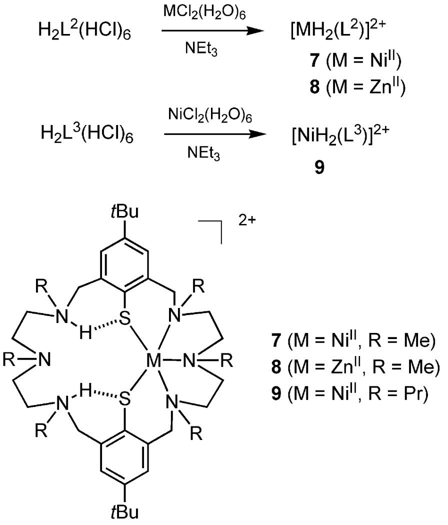

Scheme 4 Synthesis of complexes **7–9**.

The synthesis of the homodinuclear complexes **7–9** is depicted in Scheme 4. Addition of $NiCl_2{\cdot}6H_2O$ to a solution of the macrocycle $H_2L^2{\cdot}6HCl$ in methanol, followed by $LiClO_4$, yields a dark red, microcrystalline solid of $[NiH_2(L^2)][ClO_4]_2$ (**7**$[ClO_4]_2$) in ≈70% yield. Salt metathesis of monometallic **7**$[ClO_4]_2$ with $NaBPh_4$ in methanol gave **7**$[BPh_4]_2$. Complex $[ZnH_2(L^2)][ClO_4]_2$ (**8**$[ClO_4]_2$) forms as the only isolable product, when the macrocycle $H_2L^2{\cdot}6HCl$ is treated with $ZnCl_2{\cdot}6H_2O$ and NEt_3 in a 1 : 1 : 6 molar ratio in methanolic solution. Similarly, the reaction of $H_2L^3{\cdot}6HCl$ with $NiCl_2{\cdot}6H_2O$ and NEt_3 in methanol produced red $[NiH_2(L^3)]^{2+}$ (**9**), which was isolated as its tetraphenylborate salt. Again all complexes **7–9** are air-stable both in the solid state and in solution.

Preliminary experiments show that the mononuclear complexes **7** and **8** can be readily converted to homo- and heterodinuclear complexes. For example, the reaction of **7** with $Ni(OAc)_2{\cdot}4H_2O$ and triethylamine in a 1 : 1 : 2 molar ratio in hot methanol proceeded smoothly to give the known dinickel complex $[(L^{Me})Ni_2(OAc)]^+$ (**10**) in almost quantitative yield (see Scheme 5).[20] Likewise, when $[ZnH_2(L^2)]^{2+}$ (**8**) was allowed to react with $Zn(OAc)_2{\cdot}2H_2O$ and NEt_3 in methanol at room temperature, the dinuclear zinc complex $[(L^{Me})Zn_2(OAc)]^+$ (**11**) formed immediately.[20] Finally, the reaction of **8** with $Cd(OAc)_2{\cdot}2H_2O$ and NEt_3 in methanol produces a non-statistical 1 : 1 : 8 mixture (by ^1H NMR, see below) of the two homo- and the heterodinuclear $[(L^2)M^1M^2(OAc)]^+$ complexes **11** ($M^1 = M^2$ = Zn), **12** ($M^1 = M^2$ = Cd) and **13** (M^1 = Zn, M^2 = Cd), respectively. No attempt has as yet been made to further decrease the amounts of **11** and **12** in this reaction. All compounds gave satisfactory elemental analyses and were characterized by spectroscopic methods (IR, ^1H and ^{13}C NMR spectroscopy) and X-ray crystallography.

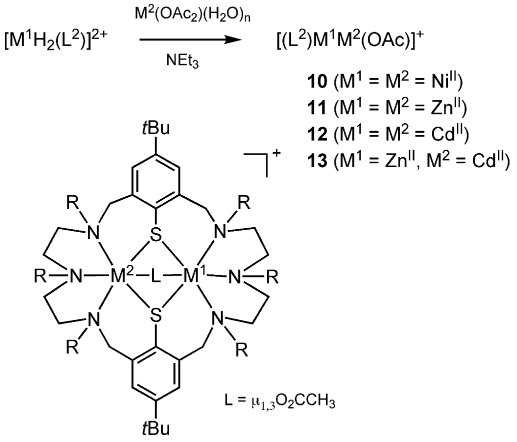

Scheme 5 Synthesis of complexes **10–13**.

Spectroscopic characterization of complexes

The most significant features in the IR spectrum of mononuclear complex **4** are the weak bands at 3046 and 3062 cm^{-1}, which can be attributed to the N–H stretching vibrations of the coordinated amine functions.[21] The IR spectra of **5** and **6** are identical, and reveal only the various stretching and bending modes of the supporting ligand. In agreement with the formulation of **7**[ClO$_4$]$_2$ and **8**[ClO$_4$]$_2$ the IR spectra display strong bands at 1100 cm^{-1} for the perchlorate anions. Absorptions due to the N–H stretching modes of the protonated R$_3$N–H$^+$ functions could not be detected. The same was true for **9**[BPh$_4$]$_2$. The IR spectrum of the heterodinuclear species **13** reveals two strong absorptions at 1582 and 1425 cm^{-1} which can be assigned to the symmetric and asymmetric stretching frequencies of a μ$_{1,3}$-bridging acetate group. Similar values were previously reported for **11**,[20] **12**,[22] and other carboxylato-bridged complexes of the type [(L^2)M$_2$(O$_2$CR)]$^+$.[23]

With the exception of the insoluble compound **4**, all Ni and Co complexes were further characterized by UV/Vis spectroscopy. The electronic absorption spectra were recorded in the range 300–1600 nm in acetonitrile solution at ambient temperature. The spectra of the intense colored nickel complexes **5**, **7**, and **9** are dominated by three strong RS$^-$ → Ni^{II} charge-transfer transitions in the 350 to 500 nm region. The weak absorptions bands above 500 nm (**5**: 771 nm, **7**: 686, 899 nm; **9**: 688, 945 nm) can be attributed to the spin-allowed d–d transitions of a five-coordinated nickel(II) ($S = 1$) ion. On the basis of these data, however, it is not possible to discriminate between a trigonal-pyramidal or a square-pyramidal coordination, for which five and six spin-allowed d–d transitions are expected.[24] The same is true for the Co^{II} complex **6**.[25]

The ^{1}H NMR spectrum of the mononuclear zinc complex **8**[ClO$_4$]$_2$ in CD$_3$CN solution shows two sharp singlets at 1.28 and 1.30 ppm corresponding to the methyl protons of two inequivalent *t*-Bu groups. The methylene and methyl protons appear as broad and overlapped resonances in the 5.4 to 1.8 ppm region. The spectrum at high δ is much better resolved, and consists of four equally intense doublet resonances at 7.39, 7.38, 7.36, and 7.35 ppm (^4J = 2.4 Hz) representing the four aromatic CH protons. The broad resonance at 8.30 ppm is tentatively assigned to the hydrogen atoms of the protonated R$_3$NH functions. The inequivalence of the *tert*-butyl groups and the four aromatic protons indicate that the solid state structure (see below) is retained in solution. As is described below the N configurations of the two benzylic nitrogen atoms bonded to the zinc are different. The two N-methyl groups at N(1) and N(2) are oriented below and above the five-membered N$_2$C$_2$Zn chelate ring (*trans* orientation), whereas the NMe groups at N(2) and N(3) are both on the same side of the chelate ring (*cis* orientation). These orientations are sensed by the *tert*-butyl groups, thereby causing their inequivalence. Finally, the fact that the cation is a monometallic species renders the two halves of each thiophenol unit to become inequivalent, such that all the four aromatic protons are in chemically different environments. The ^{13}C NMR spectrum was of little diagnostic value.

The ^{1}H NMR spectra for the C_{2v}-symmetric dizinc (**11**) and dicadmium complexes (**12**) have been reported previously.[20,22] The ^{1}H-NMR spectrum of the ZnCd derivative **13** is not a simple superposition of the spectra of **11** and **12**, a fact that is fully consistent with its heterodinuclear nature. The most salient features in the ^{1}H NMR spectra of these bowl-shaped dications are the resonances for the acetate methyl protons (see Fig. 1). As can be seen, for **11** and **12** these resonances occur at δ = 0.81 and δ = 0.98 ppm, respectively, whereas for **13** this signal is observed at δ = 0.92. This clearly reflects the heterodinuclear nature of **13**.

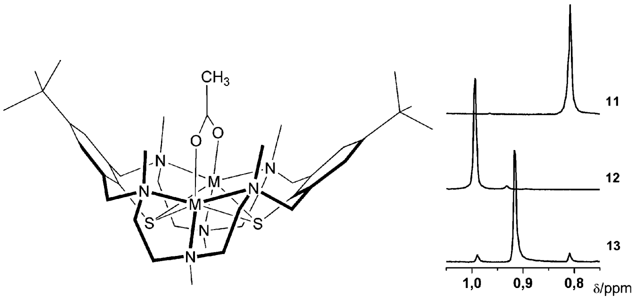

Fig. 1 Left: Schematic representation of the bowl-shaped structures of the cations **11–13**. Right: ^{1}H NMR spectra of **11**, **12**, and **13** in CD$_3$CN solution showing the resonances of the methyl protons of the bridging acetate groups in the δ = 1.0 to 0.5 ppm region. The signals at 0.81 and 0.98 ppm show that **13** is contaminated with **11** and **12** (intensity ratio: 0.8 : 0.1 : 0.1).

It should be noted that the signals for the acetate coligands are considerably shifted to high-field relative to free sodium acetate (δ = 1.83 ppm). This can be understood in terms of the ring current. As can be seen from Fig. 1, the methyl protons are positioned in the binding cavity of the complexes slightly above the center of the two phenyl rings in the shielding region. We have previously reported a correlation between the magnitude of the shielding effect and the angle between the two phenyl rings.[25,26] In the dizinc complex **11**, for example, the angle is more acute (80.0°) than in the cadmium complex **12** (94.4°) such that the distance of the methyl protons to the centre of the phenyl rings is smaller in **11** thereby causing a more pronounced shielding effect. On the basis of these data, we can estimate that the angle between the two phenyl rings in **13** is ≈87–88°.

A solution of complex **13** was also characterized by ESI-MS. The ESI-MS exhibited a strong peak at m/z = 905.3, corresponding to the [(L^2)ZnCd(μ-OAc)]$^+$ cation. Again the presence of the homodinuclear "impurities" **11** and **12** was also visible in the mass spectrum, by the weak peaks at m/z = 859.3 and 953.3. In summary, all experimental data provide sufficient evidence for the formulation of **13** as a heterodinuclear ZnCd complex coligated by a deprotonated acetate ion. Thus, the mononuclear amine-thiophenolate complexes pave the way to calixarene-like compounds with a heterobimetallic core.

Description of the crystal structures. The X-ray crystal structures of **4**, **5**, **6**, **7**$[ClO_4]_2 \cdot MeOH$, **8**$[ClO_4]_2 \cdot MeOH$, and **9**$[BPh_4]_2$ were determined to establish the geometries about the metal ions as well as the bonding modes of the supporting ligands. Experimental crystallographic data are summarized in Table 1. Selected bond lengths and angles are given in Table 2. ORTEP views of the structures of the cations are shown in Fig. 2–5. The atomic numbering scheme used for the central N_3S_2Ni core in **4** was adopted for all compounds to facilitate structural comparisons.

[Ni^{II}(L^4)] (4). The neutral complex **4** crystallizes in the monoclinic space group $P2_1/c$. The coordination geometry of the Ni atom is intermediate between trigonal bipyramidal and square pyramidal, as indicated by the τ = value of 0.44.[27] The average Ni–N and Ni–S distances of 2.086(4) and 2.318(1) Å compare well with those reported for [Ni^{II}(*terpy*)(S-2,4,6-(*i*Pr)$_3$C$_6$H$_2$)$_2$] (*terpy* = 2,2′,2″-terpyridine; Ni–N: 2.057 Å, Ni–S: 2.303 Å),[28] and other five-coordinate Ni^{II}N$_3$S$_2$ complexes.[29–32] The main difference between the structure of **4** and the compounds described below concerns the intermolecular hydrogen bonding interactions. In the present structure the individual complexes are linked *via* intermolecular N–H···S hydrogen bonds involving the thiolate sulfur atoms (S(1), S(2′)) and the amine hydrogen atoms (H(1′), H(3)) to generate one-dimensional infinite chains.[33]

Table 1 Selected crystallographic data for **4**, **5**, **6**, **7**$[ClO_4]_2 \cdot MeOH$, **7**$[BPh_4]_2 \cdot MeCN$, **8**$[ClO_4]_2 \cdot MeOH$, and **9**$[BPh_4]_2$

Compound	**4**	**5**	**6**	**7**$[ClO_4]_2 \cdot MeOH$	**7**$[BPh_4]_2 \cdot MeCN$	**8**$[ClO_4]_2 \cdot MeOH$	**9**$[BPh_4]_2$
Formula	$C_{18}H_{23}N_3NiS_2$	$C_{21}H_{29}N_3NiS_2$	$C_{21}H_{29}CoN_3S_2$	$C_{39}H_{70}Cl_2N_6NiO_9S_2$	$C_{88}H_{109}B_2N_7NiS_2$	$C_{39}H_{70}Cl_2N_6O_9S_2Zn$	$C_{98}H_{130}B_2N_6NiS_2$
M_r/g mol^{-1}	404.22	446.30	446.52	960.74	1409.27	967.40	1536.53
Space group	$P2_1/c$	$P2_1/c$	$P2_1/c$	$P2_1/n$	*Pbca*	$P2_1/n$	$P\bar{1}$
a/Å	10.799(2)	18.320(4)	18.334(4)	14.073(3)	18.177(4)	14.270(3)	14.095(3)
b/Å	13.289 (3)	7.583(2)	7.601(2)	17.070(3)	17.826(4)	16.937(3)	15.097(3)
c/Å	12.474(2)	15.183(3)	15.163(3)	19.323(4)	48.531(10)	19.708(4)	23.640(5)
α/°	90.00	90.00	90.00	90.00	90.00	90.00	89.52(3)
β/°	96.68(3)	96.70(3)	96.46(3)	93.04(3)	90.00	94.15(3)	75.64(3)
γ/°	90.00	90.00	90.00	90.00	90.00	90.00	65.07(3)
V/Å^3	1778.0(6)	2094.8(8)	2099.6(8)	4635(2)	15725(6)	4751(2)	4393(2)
Z	4	4	4	4	8	4	2
$d_{calcd.}$/g cm^{-3}	1.510	1.415	1.413	1.397	1.191	1.353	1.162
μ(Mo Kα)/mm^{-1}	1.331	1.137	1.027	0.682	0.349	0.773	0.317
θ limits/°	1.90–28.33	1.12–28.29	1.12–28.35	1.75–28.30	1.40–28.37	1.59–28.31	1.65–28.34
Measured refl.	11219	12760	12807	28635	46215	29408	40508
Independent refl.	4239	4931	4993	10921	18528	11276	20741
Observed refl.^{a}	2125	2489	3026	6237	4108	7641	8857
No. parameters	217	244	244	560	901	533	1038
$R1^b$ ($R1$ all data)	0.0507 (0.1291)	0.0524 (0.1336)	0.0481 (0.0963)	0.0463 (0.0948)	0.0566 (0.2973)	0.0523 (0.0775)	0.0457 (0.1378)
$wR2^c$ ($wR2$ all data)	0.0885 (0.1137)	0.0956 (0.1270)	0.0885 (0.1106)	0.1096 (0.1319)	0.1272 (0.2099)	0.1528 (0.1657)	0.0853 (0.1063)
Max., min. peaks/ e Å^{-3}	0.625 (−0.664)	0.644 (−0.783)	0.688 (−0.664)	0.922 (−0.610)	0.328 (−0.674)	1.563/−1.022	0.541 (−0.401)

^{a} Observation criterion: $I > 2\sigma(I)$. ^{b} $R1 = \Sigma \| F_o | - | F_c \| / \Sigma | F_o |$. ^{c} $wR2 = \{ \Sigma [w(F_o{}^2 - F_c{}^2)^2] / \Sigma [w(F_o{}^2)^2] \}^{1/2}$.

Table 2 Selected bond lengths and angles of complexes **4**–**9** and $[(L^{Et})Ni_2]^{3+}$

Compound	**4**	**5**	**6**	**7**$[ClO_4]_2$	**7**$[BPh_4]_2$	$[(L^{Et})Ni_2]^{3+}$	**8**$[ClO_4]_2$	**9**$[BPh_4]_2$
M–S(1)	2.294(1)	2.301(1)	2.269(1)	2.310(1)	2.296(2)	2.291(1)	2.3083(9)	2.304(1)
M–S(2)	2.341(1)	2.292(1)	2.298(1)	2.3041(9)	2.307(2)	2.407(1)	2.3221(9)	2.332(1)
M–N(1)	2.104(4)	2.196(4)	2.253(3)	2.159(3)	2.152(5)	2.051(3)	2.262(3)	2.137(2)
M–N(2)	2.036(3)	2.104(4)	2.130(3)	2.079(3)	2.125(5)	2.138(3)	2.103(3)	2.176(2)
M–N(3)	2.117(4)	2.275(4)	2.357(3)	2.233(3)	2.137(5)	2.060(3)	2.368(3)	2.125(2)
M–N^a	2.086(4)	2.192(4)	2.247(3)	2.157(3)	2.138(5)	2.083(3)	2.244(3)	2.146(2)
M–S^a	2.318(1)	2.297(1)	2.284(1)	2.3069(9)	2.302(2)	2.349(1)	2.3151(9)	2.318(1)
N(1)–M–N(3)	166.4(1)	162.3(1)	157.9(1)	162.9(1)	155.7(2)	145.55(12)	157.7(1)	155.72(8)
N(1)–M–S(1)	93.68(10)	96.3(1)	96.94(8)	95.61(8)	96.35(14)	100.57(9)	97.04(7)	99.96(7)
N(1)–M–S(2)	91.00(10)	92.5(1)	92.52(8)	92.77(7)	93.87(15)	92.33(9)	92.78(7)	91.26(7)
N(1)–M–N(2)	83.67(14)	82.7(1)	81.3(1)	83.4(1)	83.0(2)	85.83(13)	81.4(1)	83.33(8)
N(3)–M–S(1)	91.32(10)	96.9(1)	100.46(7)	98.42(8)	105.95(14)	113.77(10)	102.23(8)	102.76(7)
N(3)–M–S(2)	93.28(10)	93.0(1)	91.59(7)	93.14(7)	91.90(14)	94.68(10)	91.20(7)	94.19(6)
N(3)–M–N(2)	82.79(14)	82.3(1)	79.9(1)	82.7(1)	82.28(19)	85.44(13)	79.8(1)	83.25(8)
S(1)–M–S(2)	139.92(5)	113.78(6)	116.79(5)	104.42(4)	99.62(7)	82.41(4)	109.89(3)	97.37(4)
S(1)–M–N(2)	115.2(1)	106.0(1)	111.10(8)	110.03(8)	104.16(15)	100.41(9)	117.43(8)	103.25(7)
S(2)–M–N(2)	104.9(1)	140.2(1)	132.11(8)	145.54(8)	156.21(15)	176.86(9)	132.67(8)	159.29(6)
τ^b	0.44	0.37	0.43	0.29	0.01	0.52	0.41	0.06

^{a} Mean values; ^{b} τ is defined as $(\alpha - \beta)/60°$, where α = largest angle, β = second largest angle (τ = 1.0 for ideal trigonal bipyramidal; τ = 0.0 for ideal square pyramidal).

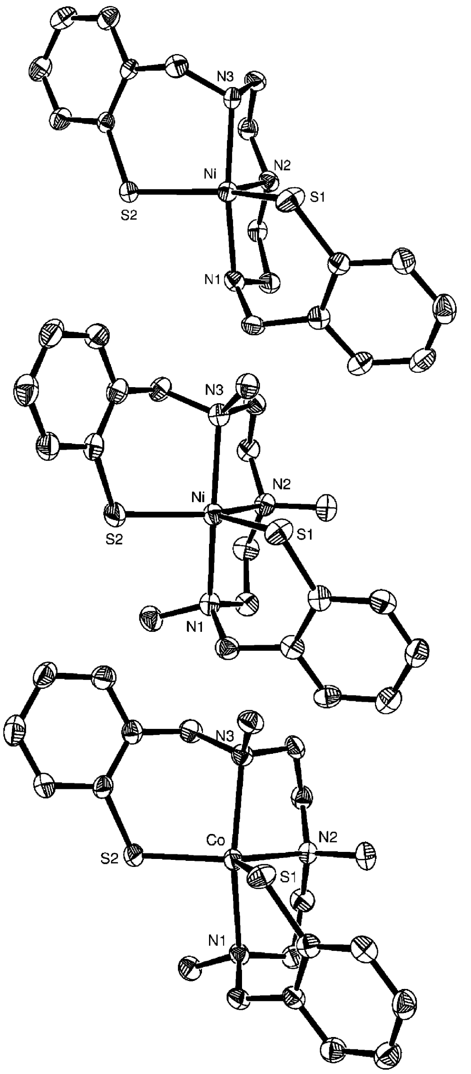

Fig. 2 Structure of the neutral complexes **4** (top), **5** (middle), and **6** (bottom). Thermal ellipsoids are drawn at the 50% probability level. Hydrogen atoms are omitted for clarity.

The corresponding distances are normal for N–H $\cdots$ S hydrogen bonds (N(1′)H(1′) $\cdots$ S(1) = 2.484 Å, N(1′) $\cdots$ S(1) = 3.297 Å, N(3)H(3) $\cdots$ S(2′) = 2.785 Å, N(3) $\cdots$ S(2′) = 3.639 Å).[34–37]

[Ni^{II}(L^5)] (5). Crystals of **5** grown from an acetonitrile solution are monoclinic space group $P2_1/c$. The crystal structure determination revealed the presence of discrete molecules of the neutral complex (Fig. 2). The conformation adopted by the permethylated ligand $(L^5)^{2-}$ resembles that of its parent $(L^4)^{2-}$ in **4**. The distortion from trigonal bipyramidal towards square pyramidal is somewhat more pronounced in **5**, as indicated by the smaller τ value of 0.37. The conversion of secondary into tertiary amines results in an increase of the average Ni–N bond distance by 0.108 Å. Similar effects have been observed for Ni complexes of other N donor ligands and their methylated derivatives.[38] The closest intermolecular distance between two complexes is observed between S(1) and a methylene carbon atom H(10′) (2.828 Å). This value should be compared with the much shorter S $\cdots$ H distances in **4**.

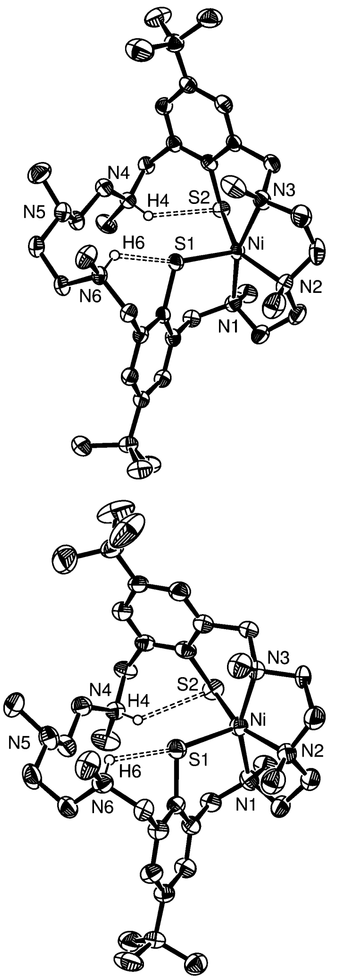

Fig. 3 ORTEP representation of the structure of complex **7** in crystals of **7**[ClO$_4$]$_2$·MeOH (top) and **7**[BPh$_4$]$_2$·MeCN (bottom). Hydrogen atoms, except H(4) and H(6), have been omitted for clarity. Selected bond lengths [Å] and angles [°] (values in square brackets refer to **7**[BPh$_4$]$_2$·MeCN): S(1) $\cdots$ H(6) 2.489 [2.612], S(1) $\cdots$ N(6) 3.153 [3.253], S(2) $\cdots$ H(4) 2.504 [2.713], S(2) $\cdots$ N(4) 3.173 [3.308]; S(1) $\cdots$ H(6)–N(6) 130.1 [128.1], S(2) $\cdots$ H(4)–N(4) 130.7 [123.9].

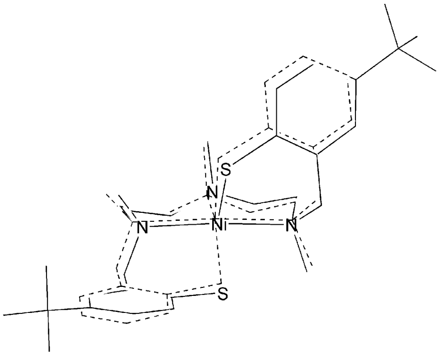

Fig. 4 Overlay of line-drawings of the structures of **5** (solid) and **7** (dashed). The noncoordinating diethylenetriamine unit of $(L^2)^{2-}$ in **7** has been omitted for clarity.

[Co^{II}(L^5)] (6). The crystal structure determination revealed **6** (Fig. 2) to be isostructural with **5**. Again, the coordination geometry for the Co atom is intermediate between trigonal

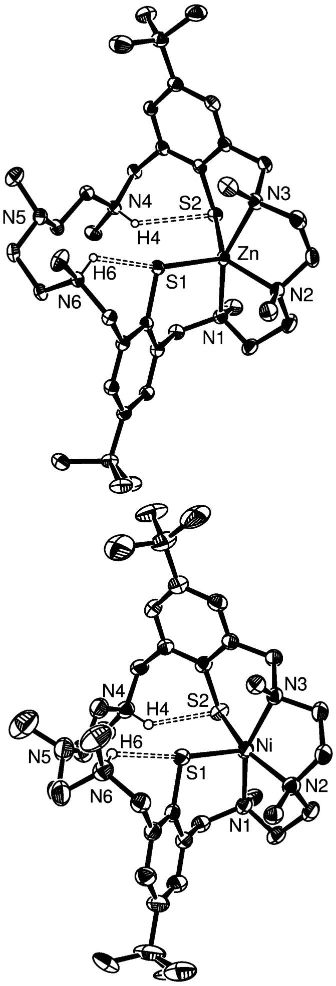

Fig. 5 ORTEP representation of the structures of complexes **8** (top) and **9** (bottom) at 50% probability ellipsoids. Hydrogen atoms, except H(4) and H(6), have been omitted for clarity. The terminal CH_3CH_2-groups of the N-propyl groups in **9** have also been omitted for reasons of clarity. Selected bond lengths [Å] and angles [°] (values in square brackets refer to **9**$[BPh_4]_2$): S(1) · · · H(6) 2.509 [2.563], S(1) · · · N(6) 3.143 [3.223], S(2) · · · H(4) 2.624 [2.354], S(2) · · · N(4) 3.262 [3.082]; S(1) · · · H(6)–N(6) 127.1 [129.9], S(2) · · · H(4)–N(4) 127.8 [137.0].

bipyramidal and square pyramidal (τ = 0.43). The distortions from the ideal trigonal bipyramidal geometry are manifested in the L–Co–L bond angles, which deviate by as much as 22.1° (N(1)–Co–N(3)) from their ideal values. The average Co–S (2.247 Å) and Co–N bond lengths (2.284 Å) are normal for five-coordinate Co(II) complexes with N_3S_2 coordination.[39] Co(III) complexes reveal much shorter bond lengths.[40,41] As expected, the metal–ligand bond lengths in **6** are larger than those in **5**. The mean difference of 0.03 Å is close to the difference of the ionic radii of the two elements (Co^{II}: 0.885 Å, Ni^{II}: 0.83 Å).[42]

$[NiH_2(L^2)][ClO_4]_2$ (7$[ClO_4]_2$). This salt crystallizes in the monoclinic space group *P*2_1*/n*. The structure contains discrete $[NiH_2(L^2)]^{2+}$ dications (Fig. 3), two perchlorate anions and a methanol molecule of solvent of crystallization. The Ni atom is five-coordinate, being coordinated by two sulfur and three nitrogen atoms. On the basis of the τ criterion (τ = 0.29), the coordination geometry is best described as distorted square pyramidal. The two hydrogen atoms H(4) and H(6) bonded to the benzylic amine nitrogens N(4) and N(6) were located unambiguously from final Fourier maps. These hydrogen atoms are intramolecularly hydrogen bonded to the thiolate sulfur atoms (S(1) · · · H(6) 2.489 Å, S(2) · · · H4 2.504 Å). A similar situation has been observed in $[CrH_2(L^2)(OAc)]^{2+}$ (S(2) · · · H(5) 2.559), the only other mononuclear transition metal complex of $(L^2)^{2-}$ that has been structurally characterized so far.[17] The average Ni–S bond lengths in **5** and **7** differ by only 0.01 Å, indicating that the bonding properties of the thiolate donors in **7** are not markedly affected by the intramolecular hydrogen bonding interactions. These values should be compared with those in the dinuclear $[Ni_2H(L^{Et})]^{3+}$ complex,[19] where the two hydrogens are displaced by a four-coordinate Ni^{II} center. The Ni–S bond distances in this compound are significantly longer (by *ca.* 0.05 Å) than in **7** (see Table 2).

It is also worth mentioning that the respective bond angles around the Ni centers in **5** and **7** are very similar. The same is true for the ligand conformations. This is illustrated in Fig. 4, representing an overlay of the line-drawings of the two structures. With the exception of the noncoordinating diethylenetriamine linker in **7**, the two structures are almost superimposable. Even the configurations of the tertiary nitrogen donors are identical. This is indicative of a rather flexible ligand backbone of $(L^2)^{2-}$ that does not confer an unusual coordination geometry on the nickel atom.

$[NiH_2(L^2)][BPh_4]_2$·MeCN (7$[BPh_4]_2$·MeCN). The crystal structure of the tetraphenylborate salt of complex **7** was also determined. Crystals of **7**$[BPh_4]_2$·MeCN grown from acetonitrile are orthorhombic space group *Pbca.* The structure contains discrete $[NiH_2(L^2)]^{2+}$ dications, two tetraphenylborate anions and acetonitrile molecules of solvent of crystallization. The conformation adopted by $(L^2)^{2-}$ in **7**$[BPh_4]_2$ is very similar to that in **7**$[ClO_4]_2$ (see Fig. 3). The most significant structural difference concerns the coordination geometry of the Ni atom. In contrast to **7**$[ClO_4]_2$ (τ = 0.29) the Ni atom in **7**$[BPh_4]_2$ reveals an almost perfect square pyramidal coordination geometry (τ = 0.01), with S(2), N(1), N(2) and N(3) forming the equatorial plane. The Ni atom lies slightly above this plane and is displaced 0.43 Å toward S(1), which constitutes the axial donor. It should be noted in this respect that five-coordinate Ni^{II} complexes are stereochemically non-rigid as the trigonal bipyramidal and square pyramidal coordination geometries are energetically close to one another.[43] This is nicely illustrated by $[Cr(en)_3][Ni(CN)_5]$.[44] In this salt there are two independent $[Ni(CN)_5]^{3-}$ ions per unit cell, one of which is a distorted trigonal bipyramid and the other a distorted square pyramid.

It should be noted that we have not been able to locate the two hydrogen atoms in the case of **7**$[BPh_4]_2$·MeCN. However, the distances between N(4) · · · S(2) at 3.308 and N(6) · · · S(1) at 3.253 Å are very similar to those in **7**$[ClO_4]_2$, indicative of protonated N(4) and N(6) donors and intramolecular N(4)–H(4) · · · S(4) and N(6)–H(6) · · · S(6) hydrogen bonds.

$[ZnH_2(L^2)][ClO_4]_2$·MeOH (8$[ClO_4]_2$·MeOH). The crystal structure of **8**$[ClO_4]_2$·MeOH consists of $[ZnH_2(L^2)]^{2+}$ complexes (Fig. 5), perchlorate anions and methanol solvate molecules. Complex **8** is isostructural with **7**. The Zn atom is five-coordinate, the coordination geometry being intermediate between trigonal bipyramidal and square pyramidal. The τ value of 0.41 is slightly higher than in **7**$[ClO_4]_2$. Again, the hydrogen atoms H(4) and H(6) are intramolecularly hydrogen bonded to the thiolate sulfur atoms, with similar S···H distances of 2.509 (S(1)···H(6)) and 2.624 Å (S(2)···H(4)). As expected, the metal–ligand bond lengths in **8** are larger than those in **7**. The mean difference of 0.03 Å is also close to the difference of the ionic radii of the two elements (Ni^{II}: 0.83 Å, Zn^{II}: 0.88 Å). It should be noted that the methyl groups bonded to N(1) and N(2) are oriented below and above the five-membered chelate ring, whereas at N(2) and N(3) they are in *trans* configuration. This situation is observed for all complexes described in this study.

$[NiH_2(L^3)][BPh_4]_2$ (9$[BPh_4]_2$). This salt crystallizes in the triclinic space group $P\bar{1}$. The structure revealed the presence of mononuclear $[NiH_2(L^3)]^{2+}$ complexes (Fig. 5) and tetraphenylborate anions. The overall structure of **9** is similar to that of **7**. Both macrocycles adopt similar conformations. The coordination geometry of the nickel is again best described as square pyramidal. This is manifested by the relatively small τ value of 0.06. The mean deviation from the plane through the equatorial atoms S(2), N(1), N(2), and N(3) is 0.004 Å. The Ni atom lies again slightly above this plane and is displaced by 0.408 Å toward S(1). Of all the complexes presented in this study **9** features the shortest S···H bonds. In particular, the short S(2)···H(4) distance at 2.354 Å and the large N(4)–H(4)···S(2) angle at 137° indicate that $NH^+\cdots S^-$ hydrogen bonding is more significant in **9**. This may be traced back to hydrophobic effects. Thus, the longer *n*-propyl groups of $(L^3)^{2-}$ create a more lipophilic microenvironment about the $NH^+\cdots S^-$ functions which in turn results in a lower local dielectric constant that strengthens the electrostatic interactions in **9**.

Conclusion

In the present study it was demonstrated that the 24-membered hexaazadithiophenolate ligands H_2L^2 and H_2L^3 support the formation of mononuclear complexes of the type $[MH_2(L)]^{2+}$. The metal atoms are five-coordinate with coordination geometries intermediate between distorted trigonal-bipyramidal and square pyramidal. Each structure is further stabilized by two intramolecular $NH^+\cdots S^-$ hydrogen bonds. A comparison with the structures of the neutral [M(L)] complexes of the open-chain N_3S_2 ligands $(L^4)^{2-}$ and $(L^5)^{2-}$ reveals that the macrocycles are rather flexible systems that do not confer unusual coordination geometries on the metal atoms. The ability of the macrocyclic complexes **8** and **9** to form homo- and heterodinuclear complexes has also been demonstrated. This sort of chemistry can now be further exploited.

Experimental

Materials and methods

All preparations were carried out under a protective atmosphere of argon. Reagent grade solvents were used throughout. 2-*tert*-Butylthiobenzaldehyde,[45] $H_2L^2\cdot 6HCl$,[46] and $H_2L^3\cdot 6HCl$,[19] were prepared as previously described. All other reagents were obtained from standard commercial sources and used without further purification. Melting points were determined in open glass capillaries and are uncorrected. Infrared spectra were recorded on a Bruker VECTOR 22 FT-IR-spectrometer. The electronic absorption spectra were measured on a Jasco V-570 UV/VIS/NIR spectrometer. ESI-FTICR mass spectra were recorded with a Bruker Apex II instrument using dilute acetonitrile solutions. Room temperature magnetic susceptibility measurements were determined with a Johnson Matthey model Mark II magnetic susceptibility balance. Elemental analyses were carried out with a VARIO EL-elemental analyzer.

CAUTION! *Perchlorate salts are potentially explosive and should therefore be prepared only in small quantities and handled with appropriate care.*

***N*,*N*″-Bis(2-*tert*-butylthiobenzyl)-diethylenetriamine (2).** To a solution of 2-*tert*-butylthiobenzaldehyde **1** (10.0 g, 51.5 mmol) in ethanol (100 mL) was added a solution of bis(2-aminoethyl)amine (2.65 g, 25.7 mmol). After the reaction mixture was stirred for 24 h, sodium borohydride (3.00 g, 79.3 mmol) was added. The reaction mixture was stirred for a further 24 h, water was added (50 mL), and the pH of the solution adjusted to 1 by addition of conc. hydrochloric acid. After all volatiles had been distilled off, the residue was taken up in 3 M aqueous potassium hydroxide solution (100 mL) and dichloromethane (100 mL). The layers were separated and the aqueous layer was extracted with dichloromethane (3 × 50 mL). The combined organic layers were washed with water (50 mL) and dried with anhydrous potassium carbonate. Evaporation of the solvent gave compound **2** as a colourless oil. This material was used in the next step without further purification (10.9 g, 92%). ^1H NMR (200 MHz, CD_3OD): $\delta = 1.27$ (s, 9 H, *t*Bu), 3.52 (s, 8 H, NCH_2CH_2N), 4.64 (s, 4 H, $ArCH_2$), 7.57 (m, 6 H, Ar*H*), 7.61 ppm (m, 2 H, Ar*H*). ^{13}C NMR (50 MHz, CD_3OD): $\delta = 32.1$ ($C(CH_3)_3$), 48.5 ($SC(CH_3)_3$), 49.4 (NCH_2), 50.0 (NCH_2), 53.5 ($ArCH_2$), 128.8, 130.9, 131.4, 133.9, 140.6, 146.3 ppm.

***N*,*N*″-Bis(2-*tert*-butylthiobenzyl)-*N*,*N*′,*N*″-trimethyl-diethylenetriamine (3).** The amine-thioether **2** (4.00 g, 8.70 mmol) was dissolved in 96% formic acid (9.02 g, 0.188 mol). To the clear solution was added a 35% aqueous solution of formaldehyde (8.74 g, 102 mmol). The reaction mixture was heated under reflux for 20 h. The reaction mixture was concentrated *in vacuo* to about 10 mL. Water (50 mL) and dichloromethane (100 mL) were added to the slicky residue, the pH of the aqueous phase was adjusted to 13 by the addition of 3 M aqueous potassium hydroxide solution and the heterogeneous mixture was stirred vigorously for 30 min. The layers were separated and the aqueous phase was extracted with dichloromethane (3 × 100 mL). The combined organic fractions were dried over K_2CO_3 and filtered. Evaporation of the solvent gave compound **3** as a colourless oil which was used in the next step without further purification (4.28 g, 98%). ^1H NMR (200 MHz, CD_3OD): $\delta = 1.16$ (s, 18 H, $C(CH_3)_3$), 2.06 (s, 6 H, NCH_3), 2.11 (s, 3 H, NCH_3), 2.46 (s, 8 H, NCH_2CH_2N), 3.76 (s, 4 H, $ArCH_2$), 7.14–7.27 (m, 4 H, Ar*H*), 7.43–7.48 ppm (m, 4 H, Ar*H*). $^{13}C\{^1H\}$ NMR (50.3 MHz, CD_3OD): $\delta = 32.2$ ($C(CH_3)_3$), 43.6 (NCH_3), 43.9 (NCH_3), 48.3 ($SC(CH_3)_3$), 56.3 (NCH_2), 56.8 (NCH_2), 61.8 ($ArCH_2$), 128.5 (CH), 130.6 (CH), 132.0 (CH), 134.6, 140.4 (CH), 145.5 ppm.

***N*,*N*″-Bis(2-mercaptobenzyl)-diethylenetriamine ($H_2L^4\cdot 3HCl$).** To a solution of sodium (3.45 g, 150.0 mmol) in liquid ammonia (150 mL) was added a solution of compound **2** (2.30 g, 5.00 mmol) in tetrahydrofuran (50 mL) dropwise at −78 °C. The resulting blue reaction mixture was stirred at −78 °C for a further 1 h to ensure complete deprotection of the thiolate functions. Solid ammonium chloride was added in small portions at −78 °C to destroy excess reducing agent. The resulting colourless suspension was allowed to warm to room temperature. After 12 h, the remaining solvent was distilled off at reduced pressure. The residue was taken up in water (50 mL) and the pH of the suspension adjusted to ≈1 to give a pale-yellow solution of H_2L^3 as the trihydrochloride salt. To remove the inorganic salts the solution was concentrated in a vacuum to a volume of ≈20 mL. Methanol (*ca.* 60 mL) was then added and the resulting solution was filtered off from NaCl and NH_4Cl. The latter two steps were repeated several times in this order, until no more salts precipitated upon addition of MeOH. Concentration of the solution afforded the title compound as a pale-yellow powder (1.55 g, 68%). ^{1}H NMR (200 MHz, D_2O/CD_3OD): $\delta = 3.32$ (m, 8 H, NCH_2CH_2N), 4.34 (s, 4 H, $ArCH_2$), 7.43–7.30 ppm (m, 8 H, ArH).

***N*,*N*″-Bis(2-mercaptobenzyl)-*N*,*N*′,*N*″-trimethyl-diethylenetriamine (H_2L^5·3HCl).** This compound was prepared by the deprotection of compound **3** (2.03 g, 4.05 mmol) with sodium (0.800 g, 34.8 mmol) in liquid ammonia (100 mL) by the procedure detailed above for H_2L^4·3HCl. The trihydrochloride salt was obtained as an impure pale-yellow powder. Nevertheless, the purity is sufficient for the preparation of the metal complexes. Yield: 1.99 g (98%). ^{1}H NMR (200 MHz, D_2O/CD_3OD): $\delta = 2.83$ (s, 6 H, NCH_3), 2.88 (s, 3 H, NCH_3), 3.69 (s, 8 H, NCH_2CH_2N), 4.47 (s, 4 H, $ArCH_2$), 7.28–7.57 ppm (m, 8 H, ArH). ^{13}C NMR (50.3 MHz, CD_3OD): $\delta = 41.5$ (NCH_3), 41.8 (NCH_3), 48.3, 54.2 (NCH_2), 54.7 (NCH_2), 60.8 ($ArCH_2$), 128.5, 130.3, 132.5, 134.7, 134.8, 135.2 ppm (ArC).

[Ni(L^4)] (4). To a solution of H_2L^4·3HCl (457 mg, 1.00 mmol) in methanol (20 mL) was added 1.00 mL of a 1.0 M solution of $NiCl_2 \cdot 6H_2O$ in methanol. To the resulting pale-green solution was added a solution of triethylamine (505 mg, 5.00 mmol) in methanol (2 mL). The resulting green solid was isolated by filtration, washed with a few mL of methanol and dried in air. An analytical sample was obtained by recrystallization from acetonitrile. Yield: 364 mg (90%). Mp 238 °C; IR (KBr, cm^{-1}): $\tilde{\nu} = 3062$(m), 3046(m) ν(N–H). UV/Vis (MeOH): λ_{max} (ε) = 352(1533), 450(1137), 660(658) nm (M^{-1} cm^{-1}). Elemental analysis (%) calcd for $C_{18}H_{23}N_3NiS_2$ (404.22): C 53.48, H 5.74, N 10.40; found: C 53.65, H 5.75, N 10.34.

[Ni(L^5)] (5). To a solution of H_2L^5·3HCl (499 mg, 1.00 mmol) in methanol (20 mL) was added 1.00 mL of a 1.0 M solution of $NiCl_2 \cdot 6H_2O$ in methanol. To the resulting pale-green solution was added a solution of triethylamine (505 mg, 5.00 mmol) in methanol (2 mL). The resulting red solid was isolated by filtration, washed with a few millilitres of methanol and dried in air. An analytical sample was obtained by recrystallization from acetonitrile. Yield: 312 mg (70%). Mp 224 °C; IR (KBr, cm^{-1}): $\tilde{\nu} = 3047$(m), 2996(s), 2964(s), 2861(s), 2809(m), 1583(w), 1557(m), 1464(s), 1433(m), 1071(m), 1036(w), 994(m), 939(m), 912(m), 818(w), 794(w), 746(m), 688(m). UV/Vis (CH_3CN): λ_{max} (ε) = 347(2456), 460(1322), 490(1324), 766(71) nm (M^{-1} cm^{-1}). Elemental analysis (%) calcd for $C_{21}H_{29}N_3NiS_2$ (446.30): C 56.51, H 6.55, N 9.42; found: C 56.49, H 6.70, N 9.44.

[Co(L^5)] (6). To a solution of H_2L^5·3HCl (499 mg, 1.00 mmol) in methanol (20 mL) was added $CoCl_2 \cdot 6H_2O$ (238 mg, 1.00 mmol). To the resulting pale-green solution was added a solution of triethylamine (505 mg, 5.00 mmol) in methanol (2 mL). The resulting green solid was isolated by filtration, washed with a few millilitres of methanol and dried in air. An analytical sample was obtained by recrystallization from acetonitrile. Yield: 287 mg (64%). Mp 224 °C; IR (KBr, cm^{-1}): $\tilde{\nu} = 3048$(m), 2991(s), 2962(s), 2857(s), 2810(m), 1583(w), 1558(m), 1463(s), 1433(m), 1069(m), 1044(m), 996(m), 941(m), 909(m), 819(w), 795(w), 747(m), 685(m). UV/Vis (CH_3CN): λ_{max} (ε) = 280 (10800), 314 (8560), 398 (3990), 596 (163), 760 (43) nm (M^{-1} cm^{-1}). Elemental analysis (%) calcd for $C_{21}H_{29}N_3NiS_2$ (446.30): C 56.51, H 6.55, N 9.42; found: C 56.49, H 6.70, N 9.44.

[NiH$_2$(L^2)][ClO$_4$]$_2$ (7[ClO$_4$]$_2$). To a suspension of H_2L^2·6HCl (500 mg, 0.562 mmol) in methanol (20 mL) was added a solution of $Ni(ClO_4)_2 \cdot 6H_2O$ (205 mg, 0.562 mmol) in methanol (5 mL). To the reaction mixture was added a solution of triethylamine (405 mg, 4.00 mmol) in methanol (2 mL). The resulting dark red solution was stirred for a further 30 min. Then $LiClO_4 \cdot 3H_2O$ (2.00 g, 12.5 mmol) was added to give a red microcrystalline solid. The precipitate was filtered and recrystallized from methanol. Large red blocks. Yield: 450 mg (86%). Mp 265–266 °C (decomp.). IR (KBr) $\tilde{\nu}$ = 3445(s), 3012(sh), 2959(s), 2905(w), 2869(m), 1629(m), 1464(s), 1396(w), 1343(sh), 1302(w), 1262(m), 1231(m), 1199 (w), 1096(vs, ν(ClO_4^-)), 976(w), 891(w), 819(w), 794(w), 624(s). UV/Vis (MeCN): λ_{max} (ε) = 341 (2673), 425 (574), 504 (758), 688 (38), 901 nm (11 M^{-1} cm^{-1}). Elemental analysis (%) calcd for $C_{38}H_{66}Cl_2N_6NiO_8S_2 \cdot 2H_2O$ (928.70 + 36.03): C 47.13, H 7.31, N 8.71, S 6.65; found: C 47.00, H 7.16, N 8.42, S 6.77. The tetraphenylborate salt, **7**[BPh$_4$]$_2$, was prepared by adding a solution of $NaBPh_4$ (180 mg, 5.26 mmol) in methanol (5 mL) to a solution of **7**[ClO$_4$]$_2$ (50 mg, 5.4 mmol) in methanol (20 mL). The resulting solid was filtered and recrystallized from acetonitrile. Yield: 55 mg (74%). Mp 239–240 °C (decomp.). Elemental analysis (%) calcd for $C_{86}H_{106}B_2N_6NiS_2$ H_2O (1368.25 + 18.02): C 74.51, H 7.85, N 6.06, S 4.63; found: C 74.51, H 8.18, N 6.58, S 4.47. IR (KBr): $\tilde{\nu}$ = 3159(w), 3120(w), 3053(s), 3036(sh), 3027 (m), 3011(w), 2999(m), 2980(m), 2965(s), 2907(m), 2868(m), 1612(w), 1580(m), 1478(s), 1455(s), 1427(m), 1395(w), 1366(m), 1297(w), 1268(w), 1227(w), 1216(w), 1200(w), 1174(w), 1149(w), 1117(w), 1074(w), 1053(m), 1032(m), 1013(w), 966(w), 949(w), 921(w), 910(w), 894(w), 883(w), 846(w), 821(w), 791(w), 732(vs) (ν(BH_4^-)), 706(s) (ν(BH_4^-)), 625(w), 613(s), 542(w), 479(w).

[ZnH$_2$(L^2)][ClO$_4$]$_2$ (8[ClO$_4$]$_2$). This compound was prepared from H_2L^2·6HCl (500 mg, 0.562 mmol), $Zn(ClO_4)_2(H_2O)_6$ (209 mg, 0.562 mmol) and triethylamine by the procedure detailed above for **7**[ClO$_4$]$_2$. Yield: 480 mg (91%). Mp 274–275 °C (decomp.). IR (KBr) $\tilde{\nu}$ = 3445(s), 3057(m), 2985(s), 2869(m), 1631(w), 1458(s), 1365(m), 1344(w), 1304(m), 1230(m), 1180(w), 1099(vs) (ν(ClO_4^-)), 969 (m), 933(m), 896(w), 808(w), 756(w), 624(s), 564(w), 533(w), 512(w), 494(w). Elemental analysis (%) calcd for $C_{38}H_{66}Cl_2N_6O_8S_2Zn \cdot H_2O$ (935.39 + 18.02): C 47.87, H 7.19, N 8.81, S 6.73; found: C 48.20, H 7.50, N 8.41, S 6.84. ^{1}H NMR (400 MHz, CD_3CN, 25 °C, TMS): $\delta = 1.28$ (s, 9 H, $ArC(CH_3)$), 1.30 (s, 9 H, $ArC(CH_3)$), 7.35 (d, $^4J = 2.4$ Hz, 1 H, ArH), 7.36 (d,

^4J = 2.4 Hz, 1 H, ArH), 7.38 (d, ^4J = 2.4 Hz, 1 H, ArH), 7.39 (d, ^4J = 2.4 Hz, 1 H, ArH), 8.30 ppm (s br, 2 H, NH). The methylene and methyl protons appear as broad and overlapped resonances in the 5.4 to 1.8 ppm region. $^{13}C\{^1H\}$ NMR (125 MHz, $CDCl_3$, 25 °C, TMS): δ = 31.75 ArC(CH$_3$), 31.79 ArC(CH$_3$), 35.23 ArC(CH$_3$), 35.25 ArC(CH$_3$), 40.68, 42.26, 42.86, 47.18, 50.24, 52.87, 53.81, 56.51, 57.44, 64.51, 65.27, 65.95, 130.29, 130.72, 132.02, 132.16, 132.37, 133.44, 141.25, 141.81, 147.92, 148.47 ppm.

[NiH$_2$(L^3)][BPh$_4$]$_2$ (9[BPh$_4$]$_2$). To a suspension of $H_2L^3\cdot 6HCl$ (106 mg, 0.100 mmol) in methanol (20 mL) was added a solution of $Ni(ClO_4)_2\cdot 6H_2O$ (36.6 mg, 0.100 mmol) in methanol (5 mL). To the reaction mixture was added a solution of triethylamine (50.5 mg, 0.500 mmol) in methanol (2 mL). The resulting dark red solution was stirred for a further 30 min. Then $LiClO_4\cdot 3H_2O$ (160 mg, 1.00 mmol) was added to give a red microcrystalline solid. The precipitate was filtered and redissolved in methanol (100 mL). To this solution was added $NaBPh_4$ (342 mg, 1.00 mmol). The resulting red solid was filtered, washed with methanol and recrystallized from acetonitrile. Fine red needles. Yield: 82 mg (53%). Mp 242–246 °C (decomp.). IR (KBr) $\tilde{\nu}$ = 3445(s), 3056(m), 2965(s), 2874(m), 1652(w), 1579(m), 1558(m), 1460(s), 1362(m), 1229(w), 1183(w), 1149(w), 1061(w), 1033(w), 1011(w), 843(w), 733(s) ($\nu(BPh_4^-)$), 704(s) ($\nu(BPh_4^-)$), 612(s). UV/Vis (MeCN): λ_{max} (ε) = 344 (2670), 428 (715), 507 (844), 688 nm (64 M^{-1} cm^{-1}). Elemental analysis (%) calcd for $C_{98}H_{130}B_2N_6NiS_2\cdot H_2O$ (1536.57 + 18.02): C 75.71, H 8.56, N 5.41, S 4.13; found: C 75.76, H 8.64, N 5.40, S 3.90.

[(L^2)Ni$_2$(μ-OAc)][ClO$_4$] (10[ClO$_4$]). To a solution of **7**[ClO$_4$]$_2$ (92.8 mg, 0.100 mmol) in methanol (20 mL) was added a solution of NEt_3 (20.2 mg, 0.200 mmol) in methanol (2 mL). To the red solution was added a solution of $Ni(OAc)_2(H_2O)_4$ (24.9 mg, 0.100) in methanol (5 mL). The reaction mixture was heated for 6 min to give a pale-green solution. The solution was concentrated *in vacuo* to *ca.* 5 mL to give a green precipitate. The solid was filtered, washed with a few mL of methanol and dried in air. Yield: 76 mg (86%). The analytical data for this compound are identical with those reported previously for **10**[ClO$_4$].[20]

[(L^2)Zn$_2$(μ-OAc)][ClO$_4$] (11[ClO$_4$]). To a solution of **8**[ClO$_4$]$_2$ (93.5 mg, 0.100 mmol) in methanol (20 mL) was added a solution of NEt_3 (20.2 mg, 0.200 mmol) in methanol (2 mL). To the colourless solution was added a solution of $Zn(OAc)_2(H_2O)_2$ (22.0 mg, 0.100) in methanol (5 mL). After the reaction mixture was stirred for 30 min, it was concentrated *in vacuo* to *ca.* 10 mL to give a colourless precipitate. The solid was filtered, washed with a few mL of methanol and dried in air. Yield: 83 mg, (92%). The analytical material for this compound are identical with those reported previously for **11**[ClO$_4$].[20]

[(L^2)ZnCd(μ-OAc)][ClO$_4$] (13[ClO$_4$]). To a solution of **8**[ClO$_4$]$_2$ (93.5 mg, 0.100 mmol) in methanol (20 mL) was added a solution of NEt_3 (20.2 mg, 0.200 mmol) in methanol (2 mL). To the colourless solution was added a solution of $Cd(OAc)_2(H_2O)_2$ (26.7 mg, 0.100) in methanol (5 mL). After the reaction mixture was stirred for 30 min, it was concentrated *in vacuo* to *ca.* 10 mL to give a colourless precipitate. The solid was filtered, washed with a few mL of methanol and dried in air. Yield: 85 mg, (90%). IR (KBr) $\tilde{\nu}$ = 3445(s), 3048(w), 3011(w), 2962(s), 2903(w), 2868(m), 2837(w), 2806(w), 1582(s) ($\nu_{as}(OAc^-)$), 1477(w), 1458(s), 1425(s) ($\nu_{sym}(OAc^-)$), 1396(w), 1364(m), 1315(w), 1293(m), 1267(m), 1233(m), 1205(m), 1169(w), 1156(w), 1117(w), 1093(vs) ($\nu(ClO_4^-)$), 1053(w), 1043(w), 1012(w), 983(w), 926(w), 910(m), 884(m), 819(m), 803(w), 746(m), 688(w), 653(w), 626(s). ^{1}H-NMR (200 MHz, CD_3CN, 25 °C, TMS): δ = 7.11 (m, 2 H, ArH), 7.10 (m, 2 H, ArH), 4.50 (d, ^2J(H,H) = 11.6 Hz, 2 H, ArCH$_2$), 4.44 (d, ^2J(H,H) = 11.6 Hz, 2 H, ArCH$_2$), 3.52 (m, 2 H, CH$_2$), 3.39 (m, 2 H, CH$_2$), 3.19 (m, 4 H, NCH$_3$), 2.87 (s, 3 H, NCH$_3$), 2.83 (s, 3 H, NCH$_3$), 2.82 (m, 4 H, CH$_2$), 2.68 (m, 4 H, ArCH$_2$), 2.43 (m, 4 H, CH$_2$), 2.42 (s, 6 H, N^{Bz}CH$_3$), 2.38 (s, 6 H, N^{Bz}CH$_3$), 1.24 (s, 18 H, CH$_3$), 0.92 ppm (s, 3 H, O$_2$CCH$_3$). ESI-MS: *m*/*z* 905.3 ([(L^3)ZnCd(μ-OAc)]$^+$; 100), 859.3 ([(L^3)Zn$_2$(μ-OAc)]$^+$; 10), 953.3 ([(L^3)Cd$_2$(μ-OAc)]$^+$; 10).

X-Ray crystallography

Crystals of **4–6**, **7**[BPh$_4$]$_2$·MeCN, and **9**[BPh$_4$]$_2$ suitable for X-ray crystallography were obtained from acetonitrile. Crystals of **7**[ClO$_4$]$_2$·MeOH and **8**[ClO$_4$]$_2$·MeOH were obtained from methanol. Crystal data and collection details are reported in Table 1. The diffraction experiments were carried out at 210(2) K on a BRUKER CCD X-ray diffractometer using Mo Kα radiation. The data were processed with SAINT[47] and corrected for absorption using SADABS.[48] Structures were solved by direct methods and refined by full-matrix least-squares on the basis of all data against F^2 using SHELXL-97.[49] H atoms were placed in calculated positions and treated isotropically using the 1.2-fold U_{iso} value of the parent atom except methyl H atoms, which were assigned the 1.5-fold U_{iso} value of the parent C atoms. All non-hydrogen atoms were refined anisotropically.

In the crystal structure of **7**[ClO$_4$]$_2$·MeOH one ClO_4^- anion was found to be disordered over two positions. The two orientations could be successfully refined by using the SADI instruction (equal Cl–O and O···O distances, respectively) implemented in the SHELXL97 program to give site occupancies of 0.57(2) (for O(5)O(6a)–O(8a)) and 0.43(2) (for O(5)O(8b)–O(11b)). No hydrogen atoms were calculated for the O and C atoms of the MeOH solvate molecules in **7**[ClO$_4$]$_2$·MeOH and **8**[ClO$_4$]$_2$·MeOH. In the crystal structure of **9**[BPh$_4$]$_2$ the *tert*-butyl groups were found to be disordered over two positions. The two orientations were also refined by using the SADI instruction (equal C–C and C···C distances, respectively) to give site occupancies of 0.61(1)/0.39(1) (for C(44a)–C(46a)/C(44b)–C(46b)) and 0.52(1)/0.48(1) for C(48a)–C(50a)/C(48b)–C(50b).

CCDC reference numbers 601289 (**4**), 601290 (**5**), 601291 (**6**), 601292 (**7**[ClO$_4$]$_2$·MeOH), 601293 (**7**[BPh$_4$]$_2$·MeCN), 601294 (**8**[ClO$_4$]$_2$·MeOH), and 601295 (**9**[BPh$_4$]$_2$)

For crystallographic data in CIF or other electronic format see DOI: 10.1039/b603740b

Acknowledgements

This work was supported by the Deutsche Forschungsgemeinschaft (project KE 585/3-1,2,3). We thank Prof. Dr H. Vahrenkamp for providing facilities for X-ray crystallographic measurements.

References

1 H. Okawa, H. Furutachi and D. E. Fenton, *Coord. Chem. Rev.*, 1998, **174**, 51–75.

2 D. Fenton, *Chem. Soc. Rev.*, 1999, **28**, 159–168.

3 R. R. Gagne, C. L. Spiro, T. J. Smith, C. A. Hamann, W. R. Thies and A. K. Shiemke, *J. Am. Chem. Soc.*, 1981, **103**, 4073–4081.

4 S. L. Lambert, C. L. Spiro, R. R. Gagne and D. N. Hendrickson, *Inorg. Chem.*, 1982, **21**, 68–72.

5 D. G. McCollum, G. P. A. Yap, A. L. Rheingold and B. Bosnich, *J. Am. Chem. Soc.*, 1996, **118**, 1365–1379.

6 N. H. Pilkington and R. Robson, *Aust. J. Chem.*, 1970, **23**, 2225–2236.

7 P. A. Vigato, S. Tamburini and D. E. Fenton, *Coord. Chem. Rev.*, 1990, **106**, 25–170.

8 A. J. Atkins, D. Black, A. J. Blake, A. Marin-Becerra, S. Parsons, L. Ruiz-Ramirez and M. Schröder, *Chem. Commun.*, 1996, 457–464.

9 (*a*) H. Okawa, J. Nishio, M. Ohba, M. Tadokoro, N. Matsumoto, M. Koikawa, S. Kida and D. E. Fenton, *Inorg. Chem.*, 1993, **32**, 2949–2957; (*b*) M. Yamami, H. Furutachi, T. Ykoyama and H. Okawa, *Inorg. Chem.*, 1998, **37**, 6832–6838.

10 M. Yonemura, Y. Matsumura, H. Furutachi, M. Ohba, H. Okawa and D. E. Fenton, *Inorg. Chem.*, 1997, **36**, 2711–2717.

11 H. He, A. E. Martell, R. J. Motekaitis and J. H. Reibenspies, *Inorg. Chem.*, 2000, **39**, 1586–1592.

12 J. Nishio, H. Okawa, S. Ohtsuka and M. Tomono, *Inorg. Chim. Acta*, 1994, **218**, 27–32.

13 (*a*) S. Brooker and P. D. Croucher, *J. Chem. Soc., Chem. Commun.*, 1995, 1493–1494; (*b*) S. Brooker and P. D. Croucher, *J. Chem. Soc., Chem. Commun.*, 1995, 2075–2076; (*c*) S. Brooker, P. D. Croucher and F. M. Roxburgh, *J. Chem. Soc., Dalton Trans.*, 1996, 3031–3037; (*d*) S. Brooker and P. D. Croucher, *Chem. Commun.*, 1997, 459–460; (*e*) S. Brooker, P. D. Croucher, T. C. Davidson, G. S. Dunbar, C. U. Beck and S. Subramanian, *Eur. J. Inorg. Chem.*, 2000, 169–179; (*f*) S. Brooker, P. D. Croucher, T. C. Davidson, G. S. Dunbar, A. J. McQuillan and G. B. Jameson, *Chem. Commun.*, 1998, 2131–2132.

14 A. C. Marr, D. J. E. Spencer and M. Schröder, *Coord. Chem. Rev.*, 2001, **219–221**, 1055–1074.

15 (*a*) A. J. Atkins, A. J. Blake and M. Schröder, *J. Chem. Soc., Chem. Commun.*, 1993, 1662–1665; (*b*) N. D. J. Branscombe, A. J. Blake, A. Marin-Becerra, W.-S. Li, S. Parsons, L. Ruiz-Ramirez and M. Schröder, *Chem. Commun.*, 1996, 2573–2574; (*c*) N. D. J. Branscombe, A. J. Atkins, A. Marin-Becerra, E. J. L. McInnes, F. E. Mabbs, J. McMaster and M. Schröder, *Chem. Commun.*, 2003, 1098–1099.

16 S. Brooker, *Coord. Chem. Rev.*, 2001, **222**, 33–56.

17 T. Glaser, Y. Journaux, G. Steinfeld, V. Lozan and B. Kersting, *Dalton Trans.*, 2006, 1738–1748.

18 B. Kersting and G. Steinfeld, *Chem. Commun.*, 2001, 1376–1377.

19 M. Gressenbuch, V. Lozan, G. Steinfeld and B. Kersting, *Eur. J. Inorg. Chem.*, 2005, 2223–2234.

20 B. Kersting, *Angew. Chem.*, 2001, **113**, 4110–4112; B. Kersting, *Angew. Chem., Int. Ed.*, 2001, **40**, 3988–3990.

21 B. Kersting and D. Siebert, *Inorg. Chem.*, 1998, **37**, 3820–3828.

22 V. Lozan and B. Kersting, *Eur. J. Inorg. Chem.*, 2005, 504–512.

23 S. Käss, T. Gregor and B. Kersting, *Angew. Chem.*, 2006, **118**, 107–110; S. Käss, T. Gregor and B. Kersting, *Angew. Chem., Int. Ed.*, 2006, **45**, 101–104.

24 (*a*) M. Ciampoli, *Inorg. Chem.*, 1966, **5**, 35–40; (*b*) R. Morassi, I. Bertini and L. Sacconi, *Coord. Chem. Rev.*, 1973, **11**, 343–387.

25 (*a*) M. Ciampoli and G. P. Speroni, *Inorg. Chem.*, 1977, **5**, 41–44; (*b*) M. Ciampoli and G. P. Speroni, *Inorg. Chem.*, 1966, **5**, 45–49.

26 J. Hausmann, S. Käss, B. Kersting, S. Klod and E. Kleinpeter, *Eur. J. Inorg. Chem.*, 2004, 4402–4411.

27 τ is defined as $(\alpha - \beta)/60°$, where α = largest angle, β = second largest angle ($\tau = 1.0$ for ideal trigonal bipyramidal; $\tau = 0.0$ for ideal square pyramidal); A. W. Addison, T. N. Rao, J. Reedijk, J. Van Rijn and G. C. Verschoor, *J. Chem. Soc., Dalton Trans.*, 1984, 1349–1356.

28 C. A. Marganian, H. Vazir, N. Baidya, M. M. Olmstead and P. K. Mascharak, *J. Am. Chem. Soc.*, 1995, **117**, 1584–1594.

29 N. Baidya, M. M. Olmstead, J. P. Whitehead, C. Bagyinka, M. J. Maroney and P. K. Mascharak, *Inorg. Chem.*, 1992, **31**, 3612–3619.

30 P. Stavropoulos, M. C. Muetterties, M. Carrie and R. H. Holm, *J. Am. Chem. Soc.*, 1991, **113**, 8485–8492.

31 (*a*) T. L. James, D. M. Smith and R. H. Holm, *Inorg. Chem.*, 1994, **33**, 4869–4877; (*b*) G. Fallani, R. Morassi and F. Zanobini, *Inorg. Chim. Acta*, 1975, **12**, 147–154; (*c*) F. Osterloh, W. Saak and S. Pohl, *J. Am. Chem. Soc.*, 1997, **119**, 5648–5656.

32 M. D. Santana, G. Garcia, A. Rufete, M. C. Ramirez de Arellano and G. Lopez, *J. Chem. Soc., Dalton Trans.*, 2000, 619–625.

33 Symmetry code used to generate equivalent atoms: x, $0.5 - y$, $-0.5 + z$.

34 J. E. Huheey, E. A. Keiter and R. L. Keiter, *Anorganische Chemie, 2. Aufl.*, Walter de Gruyter, Berlin, 1995, p. 347.

35 T. Steiner, *Angew. Chem.*, 2002, **114**, 50–80; T. Steiner, *Angew. Chem., Int. Ed.*, 2002, **41**, 48–76.

36 B. Krebs, *Angew. Chem.*, 1983, **95**, 113–134; B. Krebs, *Angew. Chem., Int. Ed. Engl.*, 1983, **22**, 113–134.

37 T. Ueno, N. Nishikawa, S. Moriyama, S. Adachi, K. Lee, T. Okamura, N. Ueyama and A. Nakamura, *Inorg. Chem.*, 1999, **38**, 1199–1210.

38 (*a*) E. K. Barefield, G. M. Freeman and D. G. VanDerveer, *Inorg. Chem.*, 1986, **25**, 552–558; (*b*) P. Chaudhuri and K. Wieghardt, *Prog. Inorg. Chem.*, 1987, **35**, 329–436.

39 T. Komuro, T. Matsuo, H. Kawaguchi and K. Tatsumi, *Inorg. Chem.*, 2003, **42**, 5340–5347.

40 I. Kung, D. Schweitzer, J. Shearer, W. D. Taylor, H. L. Jackson, S. Lovell and J. A. Kovacs, *J. Am. Chem. Soc.*, 2000, **122**, 8299–8300.

41 L. A. Tyler, J. C. Noveron, M. M. Olmstead and P. K. Mascharak, *Inorg. Chem.*, 2003, **42**, 5751–5761.

42 (*a*) R. D. Shannon and C. T. Prewitt, *Acta Crystallogr., Sect. B*, 1969, **25**, 925–946; (*b*) R. D. Shannon, *Acta Crystallogr., Sect. A*, 1976, **32**, 751–767.

43 F. A. Cotton, G. Wilkinson, C. A. Murillo and M. Bochmann, *Advanced Inorganic Chemistry*, 6th edn, John-Wiley & Sons, Weinheim, 1999, p. 13.

44 K. N. Raymond, P. W. R. Corfield and J. Ibers, *Inorg. Chem.*, 1968, **7**, 1362–1369.

45 O. Meth-Cohn and B. Tarnowski, *Synthesis*, 1978, 56–58.

46 (*a*) M. H. Klingele, G. Steinfeld and B. Kersting, *Z. Naturforsch.*, 2001, **56b**, 901–907; (*b*) G. Siedle and B. Kersting, *Z. Anorg. Allg. Chem.*, 2003, **629**, 2083–2090.

47 *SAINT+, V6.02*, Bruker AXS, Madison, WI, 1999.

48 Sheldrick, *SADABS, Area-Detector Absorption Correction*; University of Göttingen, Göttingen, Germany, 1996.

49 G. M. Sheldrick, *SHELXL-97, Computer program for crystal structure refinement*, University of Göttingen, Göttingen, Germany, 1997.